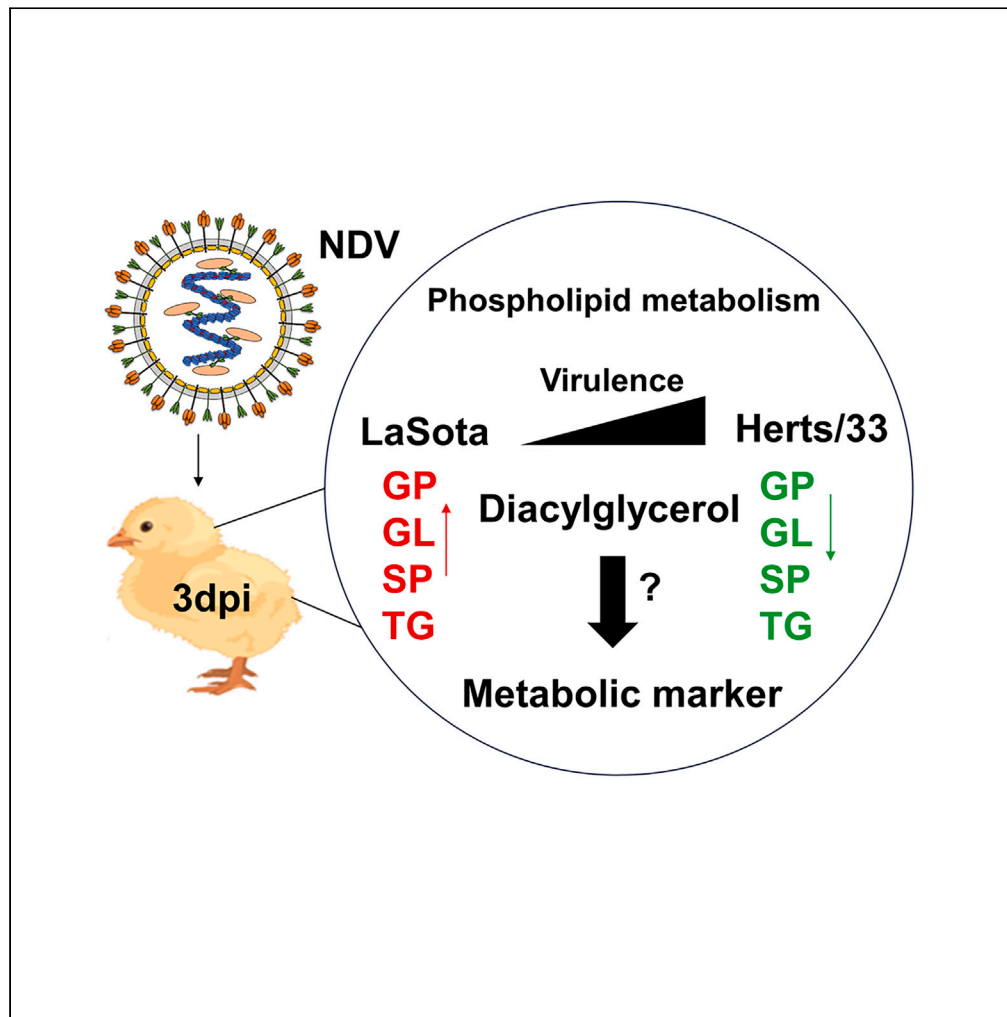


Article

Newcastle disease virus infection remodels plasma phospholipid metabolism in chickens



Jun Dai, Xusheng Qiu, Xinyuan Cui, ..., Weiwei Liu, Yongyi Shen, Chan Ding

sheny@scu.edu.cn (Y.S.)
shoveldeen@shvri.ac.cn (C.D.)

Highlights

Chicken plasma metabolic network map during NDV infection is reported for the first time

NDV preferentially targets infected blood endothelial cells in lung tissue

NDV regulate ribosome protein transcription to facilitate viral translation

NDV remodels the plasma phospholipid metabolism network in chickens

Dai et al., iScience 27, 108962
February 16, 2024 © 2024 The Authors.
<https://doi.org/10.1016/j.isci.2024.108962>



Article

Newcastle disease virus infection remodels plasma phospholipid metabolism in chickens

Jun Dai,^{1,2,5} Xusheng Qiu,^{1,5} Xinyuan Cui,³ Yiyi Feng,¹ Yuechi Hou,¹ Yingjie Sun,¹ Ying Liao,¹ Lei Tan,¹ Cuiping Song,¹ Weiwei Liu,¹ Yongyi Shen,^{3,*} and Chan Ding^{1,4,6,*}

SUMMARY

Newcastle disease is a global problem that causes huge economic losses and threatens the health and welfare of poultry. Despite the knowledge gained on the metabolic impact of NDV on cells, the extent to which infection modifies the plasma metabolic network in chickens remains unknown. Herein, we performed targeted metabolomic and lipidomic to create a plasma metabolic network map during NDV infection. Meanwhile, we used single-cell RNA sequencing to explore the heterogeneity of lung tissue cells in response to NDV infection *in vivo*. The results showed that NDV remodeled the plasma phospholipid metabolism network. NDV preferentially targets infected blood endothelial cells, antigen-presenting cells, fibroblasts, and neutrophils in lung tissue. Importantly, NDV may directly regulate ribosome protein transcription to facilitate efficient viral protein translation. In conclusion, NDV infection remodels the plasma phospholipid metabolism network in chickens. This work provides valuable insights to further understand the pathogenesis of NDV.

INTRODUCTION

Newcastle disease (ND) is a global problem that causes huge economic losses and threatens the health and welfare of poultry.^{1–3} Our previous research showed that Newcastle disease virus (NDV) activated multiple signaling pathways to facilitate viral replication and induced severe organ pathology. For instance, NDV infection modulates host cell metabolism,^{4,5} translation,⁶ stress granules,⁷ cell cycle,⁸ inflammatory response,^{9,10} mitochondrial function,¹¹ type I Interferon production,^{12–15} T lymphocyte proliferation,¹⁶ ferroptosis,¹⁷ and autophagy.^{18–20} Most of these changes are beneficial to NDV replication in chicken cells and tissues. NDV induces extensive tissue damage in the testes, brain and liver, and affects the exocrine and endocrine functions of the pancreas.^{1,21–24}

Our previous transcriptome analysis showed that the avian innate immune response induced by highly virulent NDV Herts/33 strain was significantly different from that induced by nonvirulent LaSota strain.²⁵ Genotype VII NDVs have the potential to cause differential infections in chickens and ducks.²⁶ In particular, lentogenic NDV strains circulating among poultry might be a risk for future potential velogenic NDV outbreaks in chickens.²⁷ We previously reported an *in vitro* and *in vivo* metabolomic analysis after infection with the velogenic NDV strain Herts/33 in DF-1 cells and lungs.²⁸ These studies have provided important reference for future research on the pathogenesis of NDV. Although significant progress has been made in research into the pathogenesis of NDV, the plasma metabolic changes caused by the differences in virulence between strains infection remain unclear.

In this study, we characterized the NDV infection metabolic features of chickens through integrative analyses of plasma metabolomics and lung tissue single-cell transcriptome profiling. Plasma samples were collected from chickens infected with the velogenic NDV strain Herts/33 or lentogenic NDV strain LaSota and subjected to targeted metabolomic and lipidomic analysis using an LC-MS/MS-based method. Lung tissue was collected for single-cell RNA sequencing (sc-RNA). Uninfected chicken samples were used as controls. NDV infection caused global changes in plasma metabolite profiles. These alterations were associated with differences in virulence between NDV strains. An association analysis between plasma metabolomics and sc-RNA in lung tissue revealed a correlation between plasma metabolite diacylglycerol and mRNA levels of metabolic enzymes related to pulmonary endothelial cells and interstitial cells. Additionally, selective replication of NDV in different types of chicken lung cells. These findings provide insight into the intrinsic link between host plasma metabolic changes and differences in virulence between NDV strains. These data help us to study host–virus interactions and comprehensively catalog changes in cell-type abundance after NDV infection.

¹Shanghai Veterinary Research Institute, Chinese Academy of Agricultural Sciences, Shanghai 200241, China

²Experimental Animal Center, Zunyi Medical University, Zunyi 563000, China

³Center for Emerging and Zoonotic Diseases, College of Veterinary Medicine, South China Agricultural University, Guangzhou 510642, China

⁴Jiangsu Co-innovation Center for Prevention and Control of Important Animal Infectious Diseases and Zoonoses, Yangzhou University, Yangzhou 225009, P.R. China

⁵These authors contributed equally

⁶Lead contact

*Correspondence: shenyy@scau.edu.cn (Y.S.), shovelden@shvri.ac.cn (C.D.)

<https://doi.org/10.1016/j.isci.2024.108962>



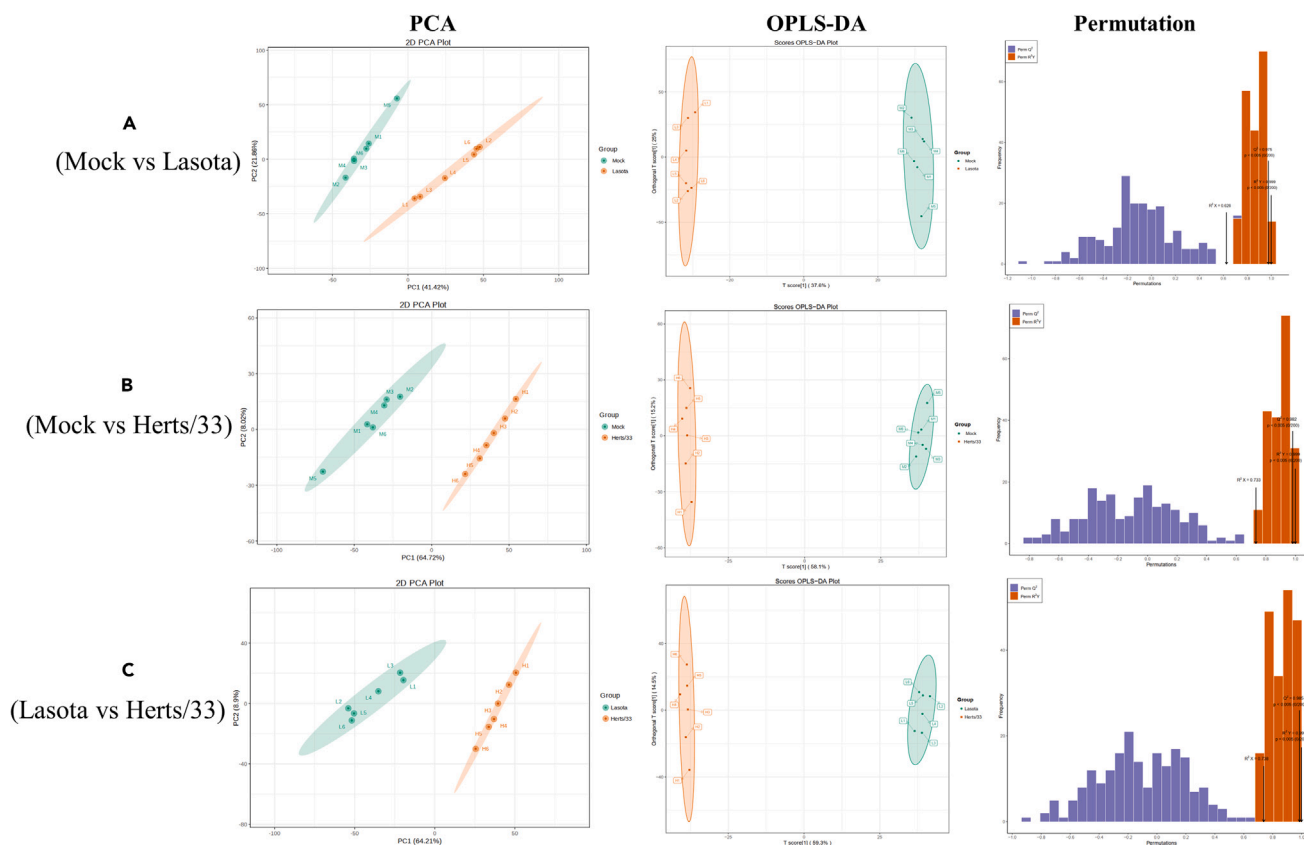


Figure 1. Multivariate analysis of chicken plasma metabolites under NDV infection

Metabolic profile of the Mock and LaSota group (A), Mock and Herts/33 group (B), LaSota and Herts/33 group (C), visualized by PCA, OPLS-DA and a permutation test. Ellipses represent 95% confidence intervals. In the principal component analysis chart, PC1 signifies the first principal component, while PC2 denotes the second principal component. The percentage indicates the explanatory power of each principal component to the dataset. Each point on the figure corresponds to a sample, with samples belonging to the same group distinguished by a consistent color. The grouping is represented by the variable named "Group". In the OPLS-DA score scatterplot, each point represents a sample, and samples with the same grouping are depicted with the same color. Group denotes the respective grouping. The horizontal axis signifies the predicted component score value, thereby displaying the distinctions between groups in that direction. The vertical axis represents the score values of orthogonal components, allowing for the visualization of differences within the group. The percentage indicates the explanatory power of the component in relation to the dataset.

RESULTS

Multivariate analysis of plasma metabolites under NDV infection

Principal component analysis (PCA) can effectively discern the overall disparities in metabolites between different sample groups, as well as assess the extent of variation within each group.²⁹ Orthogonal partial least squares discriminant analysis (OPLS-DA) is a predictive model utilized to establish the correlation between metabolite expression levels and sample categories.³⁰ In order to comprehensively acquire reliable data concerning the mock and other groups (Mock vs. LaSota, Mock vs. Herts/33, LaSota vs. Herts/33), we applied PCA and OPLS-DA analysis to analyze the chemical composition of metabolites (Figures 1A–1C). By employing the PCA and OPLS-DA model, we can evaluate whether NDV had an effect on plasma metabolic profiles. Meanwhile, we conducted a permutation test to authenticate the correctness and predictive capability of the OPLS-DA model (Figures 1A–1C). The results of PCA and OPLS-DA revealed a distinction between the mock and other groups, suggesting that NDV infection significantly altered the concentration of metabolites in the plasma, which can be exploited for further investigations.

Global changes in metabolic in response to NDV infection

Full-spectrum metabolomics technology enables us to extract hydrophilic metabolites and lipids from plasma. Our two sets of detection systems, utilizing extensive targeted technology, ensure stable detection of more than 7000 metabolites in the sample, encompassing categories such as amino acids, organic acids, nucleic acids, carbohydrates, sterols, fatty acids, sphingolipids, glycerides, phospholipids, coenzymes and vitamins (Figure 2A). The analysis of plasma metabolites revealed that 21 different categories of metabolites were detected, with glycerol phospholipids, glycerol lipids, amino acids and their metabolites, sphingolipids and organic acids and their derivatives being the

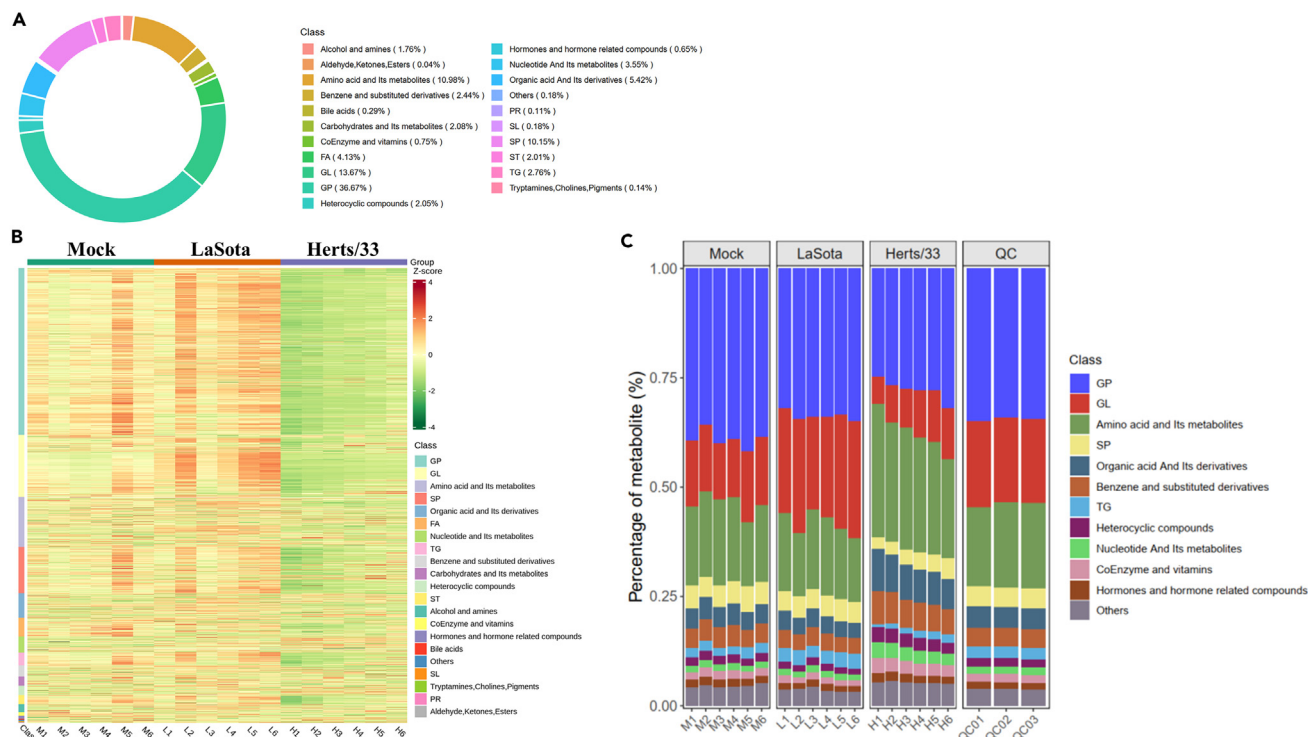


Figure 2. Global Changes in Metabolic in Response to NDV Infection

(A) The metabolite categories form a circular graph, with each color representing a metabolite category, and the area of the color block represents the proportion of that category.

(B) Heatmap of metabolite content. Horizontal represents the sample name, vertical represents the metabolite classification, Group represents grouping, red represents high content, green represents low content, and class represents the primary classification of the substance.

(C) Percentage of metabolite content in each sample.

most abundant (Figures 2A and 2B). NDV infection led to comprehensive changes in these categories of metabolites (Figure 2B). To more clearly show the influence of NDV infection on these metabolites, we calculated the proportion of various metabolites in each group (Figure 2C). In summary, the changes in these metabolites caused by NDV infection were found to be closely related to phospholipid metabolism.

K-means cluster analysis of differential plasma metabolites

To determine the trend of different plasma metabolites under NDV infection, 1468 co-expressed metabolites were analyzed using K-means cluster analysis (Figure 3). The analysis revealed 4 distinct categories, with 200, 504, 62, and 702 metabolites clustered in categories 1 to 4, respectively. Notably, NDV infection leads to the category 1 exhibited a continual decline in their content. The most differential plasma metabolites in class 1, class2 and class4 were belonged to GP, GL, and SP. Moreover, the majority of differential plasma metabolites in class3 were from nucleotide and its metabolites, organic acid and its metabolites, and amino acid and its metabolites. Identifying the common and unique differential plasma metabolites induced by velogenic NDV strain Herts/33 or lentogenic NDV strain LaSota was of utmost importance for studying the pathogenesis of NDV. Therefore, we conducted a volcano plot and Venn diagram analysis of significant differential plasma metabolites between Mock vs. LaSota, Mock vs. Herts/33, and LaSota vs. Herts/33 (Figure 4). Venn diagram analysis revealed that 246 metabolites shared by all groups, highlighting the metabolic variations following infection with varying NDV virulence strains (Figure 4D).

NDV strain LaSota upregulates plasma phospholipid metabolites

To better comprehend the effects of NDV infection on plasma metabolism, we conducted a global lipidomic survey of chicken plasma infected with lentogenic NDV strain LaSota for 3 days. Lipids that were extracted from populations of both mock and infected chicken plasma ($n = 6$ biological replicates for each group) were analyzed using UPLC-MS/MS. A total of 381 plasma metabolites (319 up-regulated, 62 down-regulated) significantly changed after LaSota infection (Figure 5A). The lists of differentially plasma enriched metabolites are shown in Table S1, and were visualized via a volcano plot (Figure 4A). Most of these differential plasma metabolites are lipid molecules that take part in different lipid metabolism pathways, such as contributing to the regulation of lipolysis in adipocytes, cholesterol metabolism, glycerolipid metabolism, fat digestion and absorption, and vitamin digestion and absorption (Figure 5B). To clearly observe the alterations in the relative content of metabolites caused by LaSota, we applied Unit Variance Scaling treatment to the original content of the differential

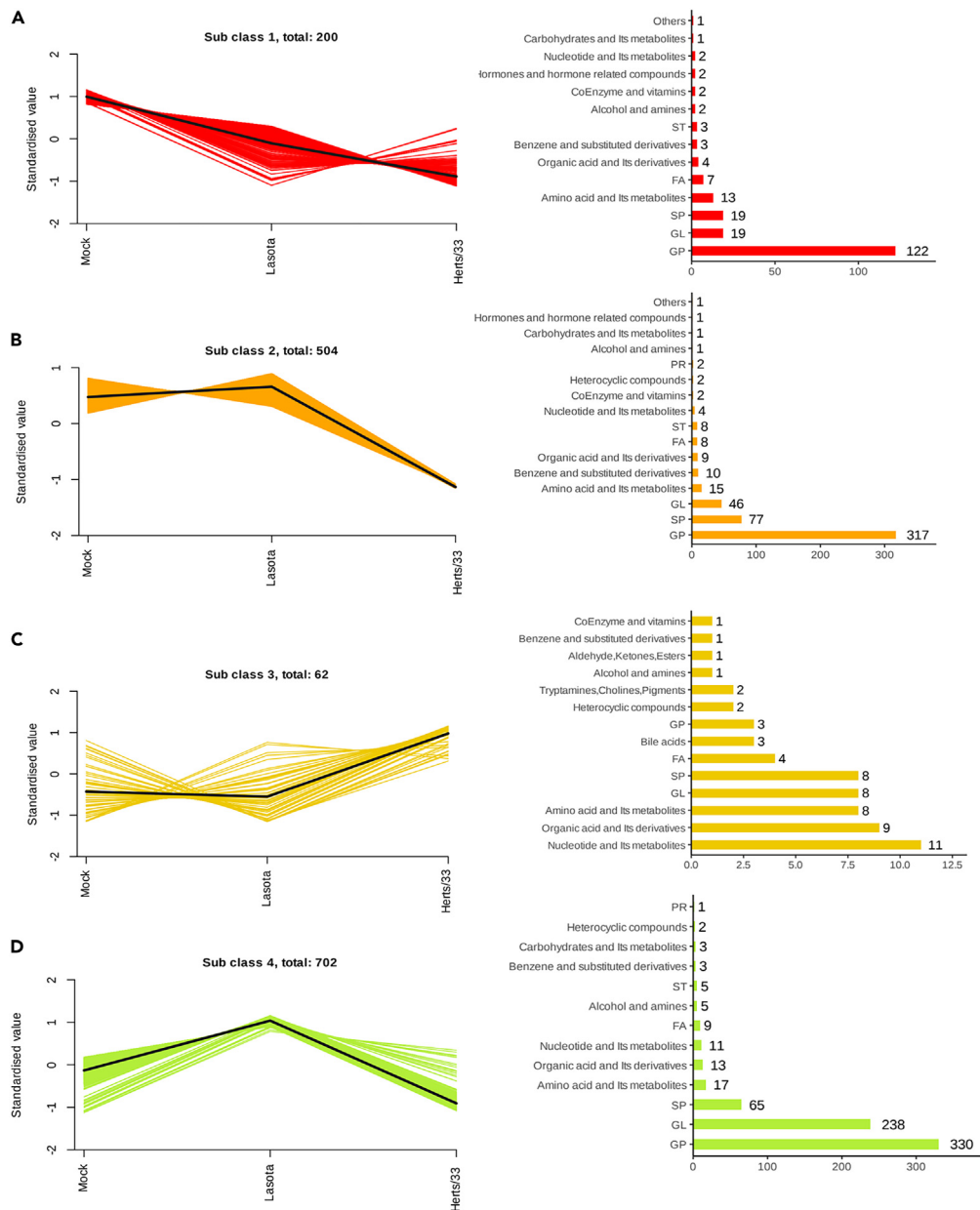


Figure 3. K-means cluster analysis of differential plasma metabolites

The K-means cluster analysis revealed 4 distinct categories, with 200 (A), 504 (B), 62 (C), and 702 (D) metabolites clustered in categories 1 to 4, respectively. The horizontal axis represents the sample group, while the vertical axis corresponds to the standardized relative content of metabolites. "Sub class" denotes the number of metabolite classes exhibiting similar patterns of change, while "total" indicates the count of metabolites within that category.

metabolites in rows and produced a heatmap using the R software package. Metabolites such as glycerolipids, glycerophospholipids, sphingolipids, and triglyceride in the plasma of chickens infected with LaSota were significantly upregulated (Figures 5C and 5D).

NDV strain Herts/33 downregulates plasma phospholipid metabolites

To assess whether the metabolic changes induced by Herts/33 were distinct from those of LaSota, we compared their metabolic profiles using PCA and OPLA-DA. The results revealed a clear segregation between the Herts/33 and Mock or LaSota groups (Figures 1B and 1C), indicating that Herts/33 elicited significant modifications in the concentrations of metabolites in the plasma. A total of 1197 plasma metabolites (42 up-regulated, 1155 down-regulated) significantly changed after Herts/33 infection (Figure 5A). The lists of differentially enriched metabolites are presented in Table S2 (Mock vs. Herts/33) and Table S3 (LaSota vs. Herts/33), along with the volcano plots (Figures 4B and 4C). After infection

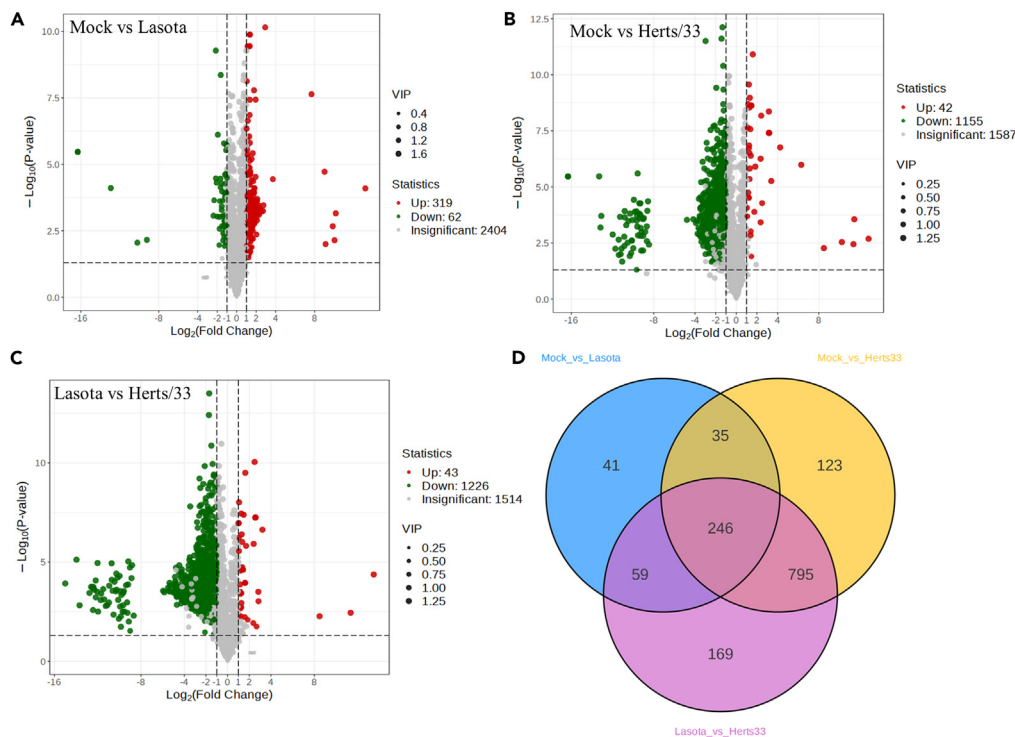


Figure 4. Significant differential plasma metabolites during NDV infection

(A) Volcano plots for the Mock and LaSota group.

(B) Volcano plots for the Mock and Herts/33 groups.

(C) Volcano plots for the LaSota and Herts/33 group. Each point in the volcanic map represents a metabolite. Red: upregulation; blue: downregulation; gray: not significant.

(D) Plasma metabolite changes were further examined with a Venn diagram.

with Herts/33, Class II identification revealed a significant decrease in the differential enrichment of plasma metabolites, including glycerophospholipids, glycerol phospholipids, sphingolipids, and amino acid metabolites (Figures 6A–6C). KEGG enrichment analysis indicated that these differentially enriched metabolites were linked to multiple metabolic pathways, such as glycerophospholipid metabolism, choline metabolism, cholesterol metabolism, glycerolipid metabolism, fat digestion and absorption, thermogenesis, and vitamin digestion and absorption (Figure 6B). These alterations in plasma metabolism likely explain the variance in the level of NDV replication in chickens.

The GP-GL-SP network is a key determinant of NDV infection

Our findings suggest that there is a close connection between NDV infection and phospholipid metabolism in plasma, as demonstrated by the opposite trends of glycerophospholipids–glycerolipids–sphingolipids (GP-GL-SP) observed during infection with the NDV strains Herts/33 and LaSota (Figures 5C and 6A). This led us to further explore the relationship between NDV and phospholipid metabolism. First, we use differential metabolite clustering heat maps to illustrate changes in relative metabolite content between Herts/33 and LaSota (Figure 7A). These differentially enriched metabolites were linked to multiple metabolic pathways, such as glycerophospholipid metabolism, glycerolipid metabolism, regulation of lipolysis in adipocytes, fat digestion and absorption, cholesterol metabolism, and vitamin digestion and absorption (Figure 7A). Next, we examined how Herts/33-induced changes in host GP-GL-SP composition broke down by subclass and species in our dataset, compared to LaSota (Figure 7B). Herts/33 infection caused a comprehensive downregulation of the GP-GL-SP compounds in the plasma of chicks (Figure 7B). Venn diagram showed that chickens infected with Herts/33 and LaSota shared 281 differential metabolites, compared with the mock (Figure 7C). The top 50 metabolites, which were downregulated by Herts/33, were significantly upregulated by LaSota out of the 281 differentially expressed metabolites (Figure 7D). In summary, Herts/33 and LaSota led to opposite trends in the differential metabolites present in plasma phospholipid metabolism.

Selective replication of NDV in different types of chicken lung cells

To generate a comprehensive single-cell atlas of NDV, we isolated six lung samples from SPF chickens infected with velogenic Herts/33 strain or lentogenic LaSota strain of NDV, at 3 days post-infection (dpi). Single-cell suspensions from the lungs were processed through the 10× Genomics platform for sc-RNA, which profiles all polyadenylated mRNAs (see Figure S1). The detailed steps and methods of sc-RNA can be found in our previous study.³¹ t-SNE visualization of cells from the lungs, with 15 distinct clusters colored. Colored cells include endothelial,

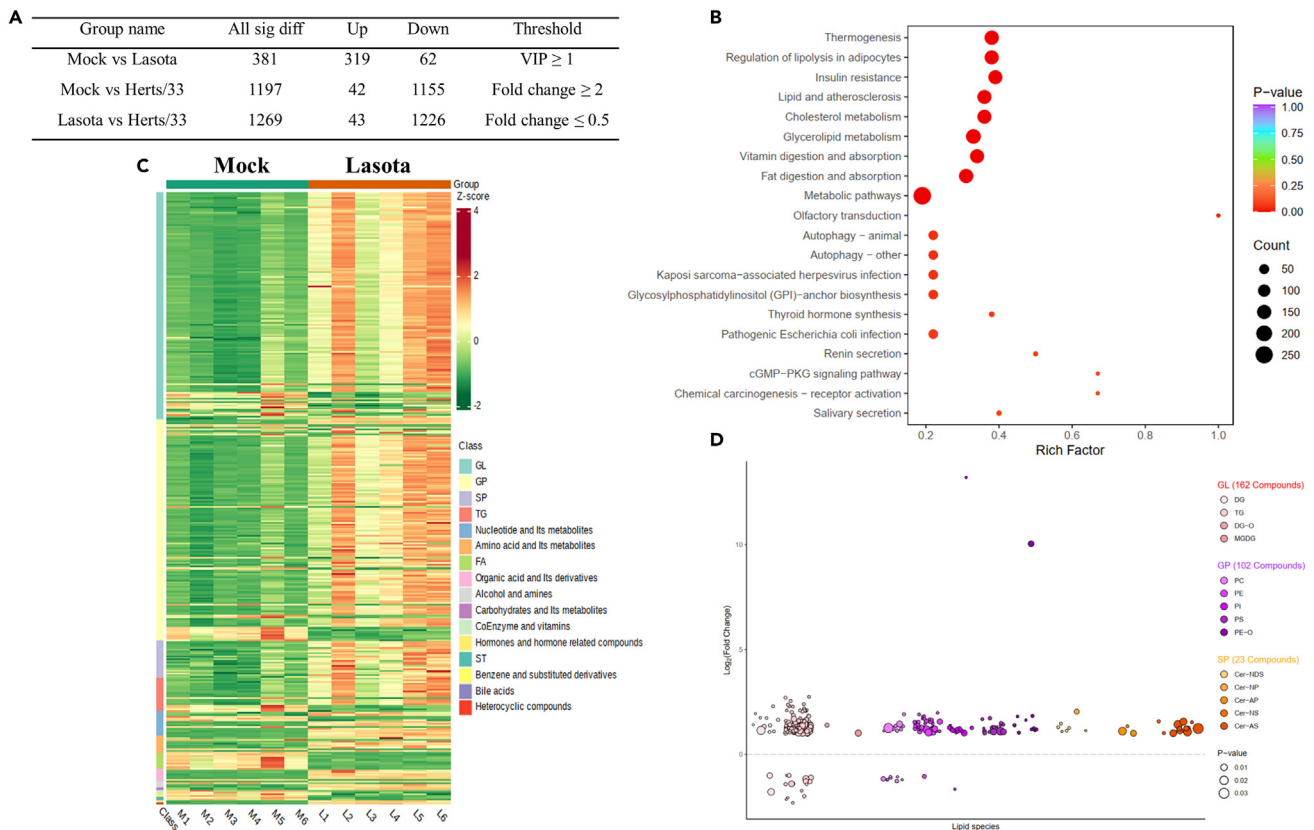


Figure 5. LaSota upregulates host plasma phospholipid metabolites

(A) Statistics of plasma differential metabolites in chickens infected with NDV, see Table S1.

(B) KEGG enrichment analysis of plasma differential metabolites (Mock vs. LaSota). The horizontal axis depicts the rich factor for each pathway, with the pathway name being indicated on the vertical axis. The significance of the enrichment is reflected by the color of the point, with redder points indicating higher significance (as dictated by P-value). The size of the point corresponds to the number of enriched differential metabolites.

(C) Differential plasma metabolites content heatmap. Horizontal represents the sample name, vertical represents the metabolite classification, Group represents grouping, red represents high content, green represents low content, and class represents the primary classification of the substance.

(D) Bubble plots of log₂ fold changes in abundance of lipid species in LaSota-infected chicken plasma relative to Mock at 3 hpi.

epithelial, and immune cells, platelets, mesenchymal cells, and neurons (Figure 8A). The percentage of different cell populations in each group is shown in Figure 8B. The transcript counts in these cells is visualized in Figure 8C. Statistical analysis was conducted to investigate whether there were any differences in the replication levels of NDV in various types of cells. Blood endothelial cells, antigen-presenting cells, fibroblasts, and neutrophils had the highest NP expression levels of Herts/33 compared to other cell types (Figures 8D–8F). This indicates that NDV replication had a selectivity for different types of lung cells. NDV preferentially targets infected blood endothelial cells, antigen-presenting cells, and mesenchymal-fibroblasts in lung tissue.

NDV regulating transcription of ribosomal proteins to remodel ribosomes

To comprehensively evaluate the effect of Herts/33 infection on cell transcription *in vivo*, we conducted KEGG enrichment analysis on differentially expressed genes of six cell types - fibroblasts, antigen-presenting cells, and blood endothelial cells with active replication of Herts/33, and lymphatic endothelial cells, natural killer cells, and neuron cells with inactive replication of Herts/33. NDV infection generally inhibits host biosynthesis and metabolic activity (Figure 9). Viral infection significantly down-regulated ribosome protein transcription in many cell types, but some genes involved in ribosome biosynthesis were up-regulated, indicating that NDV directly regulated ribosome protein transcription to facilitate efficient viral protein translation. This phenomenon was observed across different cell types and was not restricted to viral titers.

Associations of transcriptome and plasma metabolome

We further investigated the associations between single cell transcriptome and plasma metabolome in chickens, which could potentially help shed light on the pathogenesis of NDV. We assessed the effect of fibroblast cells (Figure 10A), epithelium cells (Figure 10B), and blood endothelial cells (Figure 10C) single cell transcriptome on the plasma metabolome, using Wilcoxon-test. Levels of sphingomyelin, glucosylceramide,

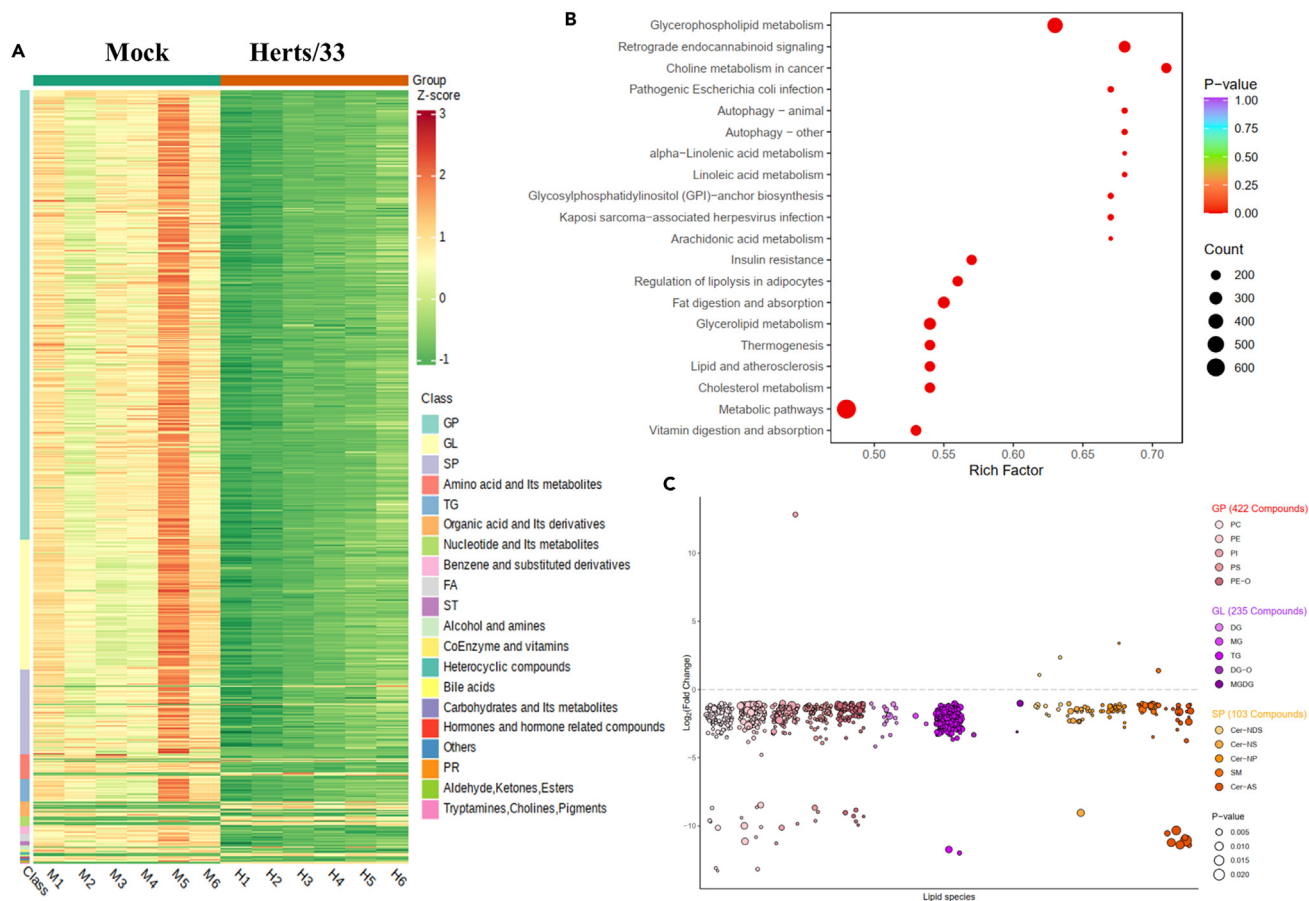


Figure 6. NDV strain Herts/33 downregulates plasma phospholipid metabolites

(A) Differential plasma metabolites content heatmap. Horizontal represents the sample name, vertical represents the metabolite classification, Group represents grouping, red represents high content, green represents low content, and class represents the primary classification of the substance, see Table S2.

(B) KEGG enrichment analysis of plasma differential metabolites (Mock vs. Herts/33). The horizontal axis depicts the rich factor for each pathway, with the pathway name being indicated on the vertical axis. The significance of the enrichment is reflected by the color of the point, with redder points indicating higher significance (as dictated by P-value).

(C) Bubble plots of log₂ fold changes in abundance of lipid species in Herts/33-infected chicken plasma relative to mock at 3 hpi.

sulfatide, triacylglycerol, phosphatidylcholine, phosphatidylserine, phosphatidate, and acylglycerol in the plasma were closely related to host mRNA levels of metabolic enzymes in pulmonary endothelial cells and interstitial cells. KEGG enrichment analysis showed that Herts/33 infection resulted in significant downregulation of metabolites related to glycerolipid metabolism (# gga00561) (Figure 10D), sphingolipid metabolism (# gga00600) (Figure 10E), and glycerophospholipid metabolism (# gga00564) (Figure 10F) in blood endothelial cells, which correlated with the mRNA levels of related metabolite enzymes. As expected, significant changes in phospholipid metabolites caused by NDV infection, including glycerolipid, sphingolipids and glycerophospholipids, had a strong significant correlation with the single cell transcriptome in blood endothelial cells. These results suggest that plasma metabolites serve as potential biomarkers for understanding metabolic changes in lung tissue after NDV infection. Future studies may further elucidate the underlying mechanisms and potential clinical implications of these findings.

Diglyceride as potential metabolic markers for NDV infection

We explored whether there was a correlation between plasma metabolites and the level of metabolic enzyme mRNA in lung tissue after NDV infection in chickens. The hypergeometric test was used to determine the correlation between plasma metabolites and mRNA in lung histiocytes. There was a correlation between the plasma metabolite diglyceride and the mRNA levels of related metabolic enzymes in pulmonary endothelial cells and interstitial cells (Figure 11). Based on this evidence, it can be inferred that when chicken cells are infected with highly virulent strains of Herts/33, there is a comprehensive downregulation of differentially expressed genes (DGs) in their plasma. Conversely, in response to infection with the nonvirulent LaSota strain, it appears to be a compensatory upregulation of DGs. This significant alteration in plasma metabolism may serve as a distinctive characteristic of infections caused by various NDV strains exhibiting different levels of virulence. In summary, diglyceride as potential metabolic markers for NDV infection.

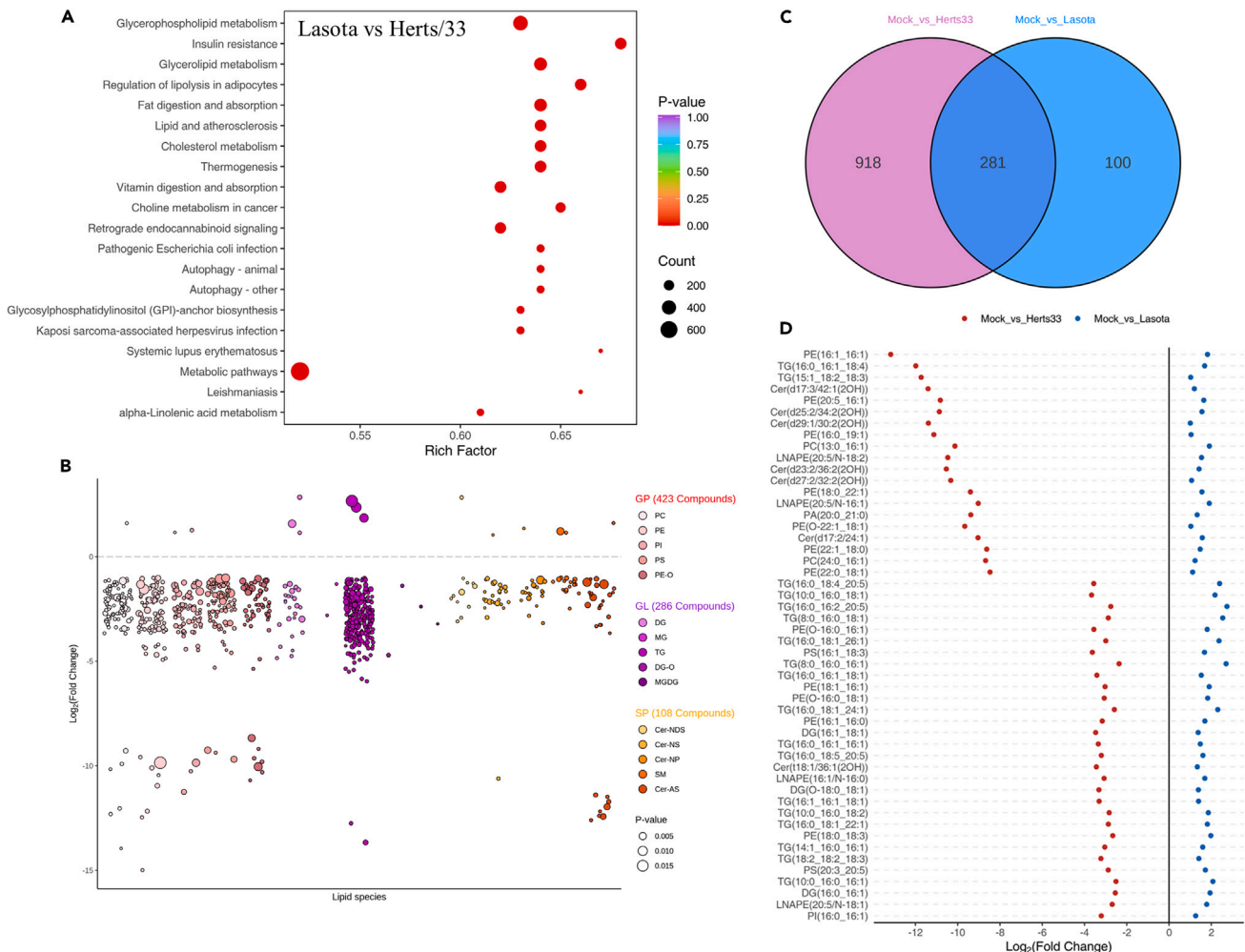


Figure 7. The GP-GL-SP network is a key determinant of NDV infection

(A) KEGG enrichment analysis of plasma differential metabolites (LaSota vs. Herts/33), see Table S3. The horizontal axis depicts the rich factor for each pathway, with the pathway name being indicated on the vertical axis. The significance of the enrichment is reflected by the color of the point, with redder points indicating higher significance (as dictated by P-value).

(B) Bubble plots of log₂ fold changes in abundance of lipid species in Herts/33-infected chicken plasma relative to LaSota group at 3 hpi.

(C) Plasma metabolite changes were further examined with a Venn diagram after NDV infection.

(D) Compared with the Mock group, the top 50 metabolites downregulated by Herts/33 infection were significantly upregulated in the La Sota group.

DISCUSSION

As a member of the *Paramyxoviridae* group, NDV is the key causative agent of ND that affects chickens, turkeys and other birds.³² ND is a global issue that results in significant economic losses and poses a threat to the health and welfare of poultry.^{33,34} It is widely accepted that the pathogenicity of the NDV virus varies with its virulence.²⁵ In comparison to a non-virulent NDV, virulent Newcastle disease virus elicits a strong innate immune response in chickens, these results suggest that the host response itself may contribute to the pathogenesis of this highly virulent strain in chickens.^{35,36} We conducted in-depth research on the pathogenesis of NDV in our prior studies, yet the molecular regulatory mechanisms of chickens' responses to NDV infection have yet to be fully elucidated.^{4-14,16-20} Specifically, our prior research demonstrated considerable differences in host transcriptional level changes provoked by NDV strains of different virulence levels, which may be attributed to disparities in pathogenicity between virulent and non-virulent strains.²⁵ There are significant differences in the expression levels of antiviral genes induced by NDV strains with different virulence levels.³⁷

Metabolomics has been widely used to investigate the responses in chickens to infection with nephropathogenic infectious bronchitis virus,^{38,39} infectious bursal disease virus,⁴⁰ Avian leukosis virus subgroup J,⁴¹ avian infectious laryngotracheitis virus,⁴² avian infectious bronchitis virus,^{43,44} and NDV.²⁸ We previously have reported the transcriptomic and metabolomic profiles following infection with NDV, both *in vitro* and *in vivo*.^{25,28,31} Currently, there are no reports on the alterations in plasma metabolic levels induced by NDV in chickens, and the interaction between distinct virulent strains of NDV and host plasma metabolites remains unknown. To explore this knowledge gap, we conducted a

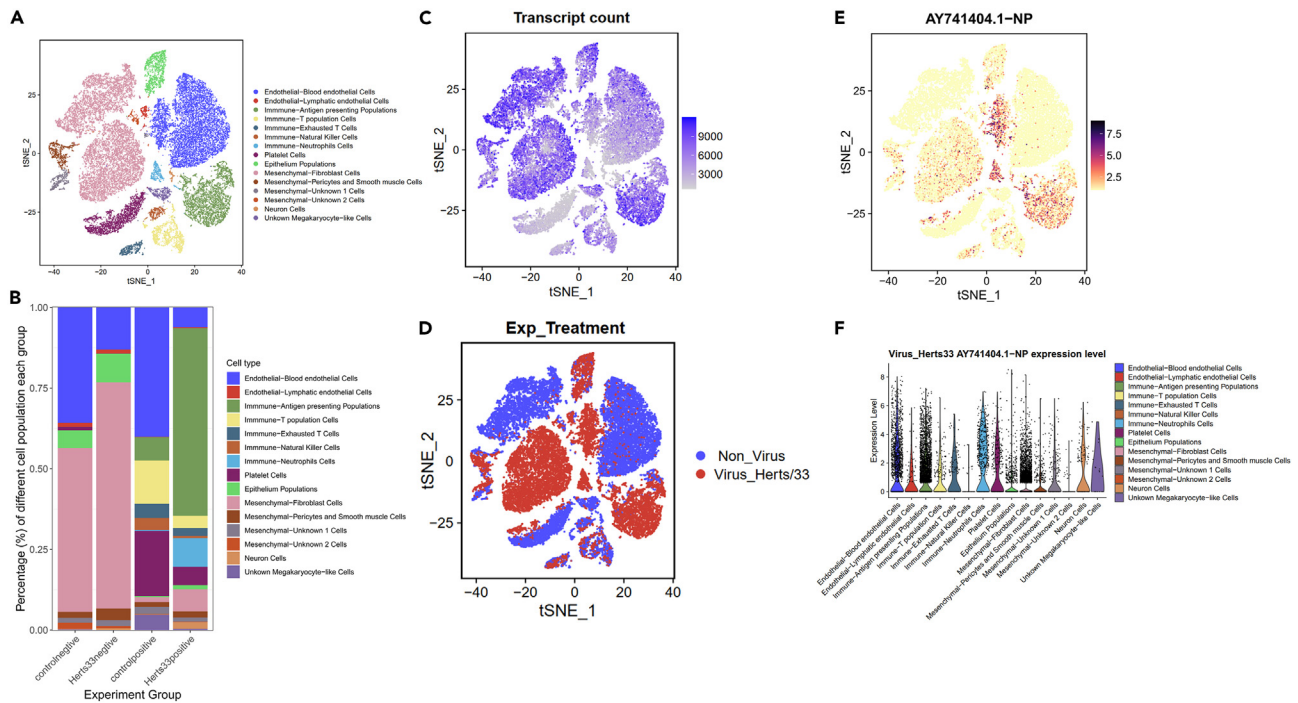


Figure 8. Selective replication of NDV in different types of chicken lung cells

- (A) t-SNE visualization of lung cells showing 15 distinct clusters with corresponding colors.
- (B) Percentage of different cell populations in each group.
- (C) Transcript counts (UMIs) in various cell types (D) t-SNE visualization of cells from the lungs, with two distinct clusters colored. Herts/33 Challenge group colored red and Control group colored blue.
- (E) The abundance of Herts/33 (GenBank: AY741404.1) infection in different types of cells in the lungs. The number represents the logarithm of relative abundance.
- (F) NP gene expression levels after infection with Herts/33 in different types of lung cells.

comprehensive lipidomic survey on the plasma of chickens infected with the velogenic NDV strain Herts/33 or lentogenic NDV strain LaSota. To our knowledge, this is the first report to create a plasma metabolic network map during NDV infection. We found that NDV infection remodels the plasma phospholipid metabolism network in chickens. The Herts/33 strain significantly reduced the production of ceramide, diacylglycerol, triglyceride, sphingomyelin, phosphatidylcholine, phosphatidylethanolamine, phosphatidylinositol, phosphatidylserine, and phosphatidic acid and other lipid molecules. In contrast, the LaSota strain induced significant upregulation of these substances. Importantly, there was a correlation between the plasma metabolite diglyceride and the mRNA levels of related metabolic enzymes in pulmonary endothelial cells and interstitial cells (Figure 11), and diglyceride maybe as a potential metabolic marker for NDV infection. In general, there exists a positive correlation between host lipid metabolism activity and virus release.⁴⁵ In our previous study, we discovered that several the highly virulent strains of NDV, including Herts/33, possess R247K mutations in their M protein.⁴⁶ Notably, these strains exhibit a faster rate of virus release due to the R247K mutations compared to the nonvirulent LaSota strain. We believe that the highly virulent strains of Herts/33 cause a rapid decline in the consumption of host lipid metabolites. Conversely, the nonvirulent LaSota strain triggers compensatory regulation of lipid metabolism, resulting in an increase. In brief, Herts/33 infection induces a substantial degradation of diglyceride (DG). These degraded DGs are utilized for the synthesis of glycerol sphingolipids, which play a crucial role as essential lipid components for viral envelope synthesis in progeny viruses.⁴⁷ Such changes in the levels of these metabolites, likely resulting from NDV targeting and interference with phospholipid metabolism in the chicken plasma, may benefit viral replication. In conclusion, we have mapped out a host-virus wiring diagram of plasma phospholipid metabolism.

Viruses lack a self-contained metabolic network. Hence, they have evolved multiple mechanisms for rewiring the metabolic system of their host to hijack the host's metabolic resources for replication. Our previous research showed that NDV remodels nucleotide metabolism,⁵ glutamine metabolism,⁴⁸ glucose metabolism,¹² iron metabolism¹⁷ and amino acid metabolism²⁸ to support self-replication. We showed here that NDV remodels plasma phospholipid metabolism, indicating a causal relationship between NDV virulence differences and phospholipid homeostasis disorders, and the phospholipid network as contributing to the molecular processes underlying NDV virulence. Sphingolipids are major components of cellular membranes, and at steady-state level, their metabolic fluxes are tightly controlled. On challenge by external signals, they undergo rapid turnover, which substantially affects the biophysical properties of membrane lipid and protein compartments and, consequently, signaling and morphodynamics.⁴⁹ Currently, our findings indicate that NDV infection leads to a significant depletion of lipids,

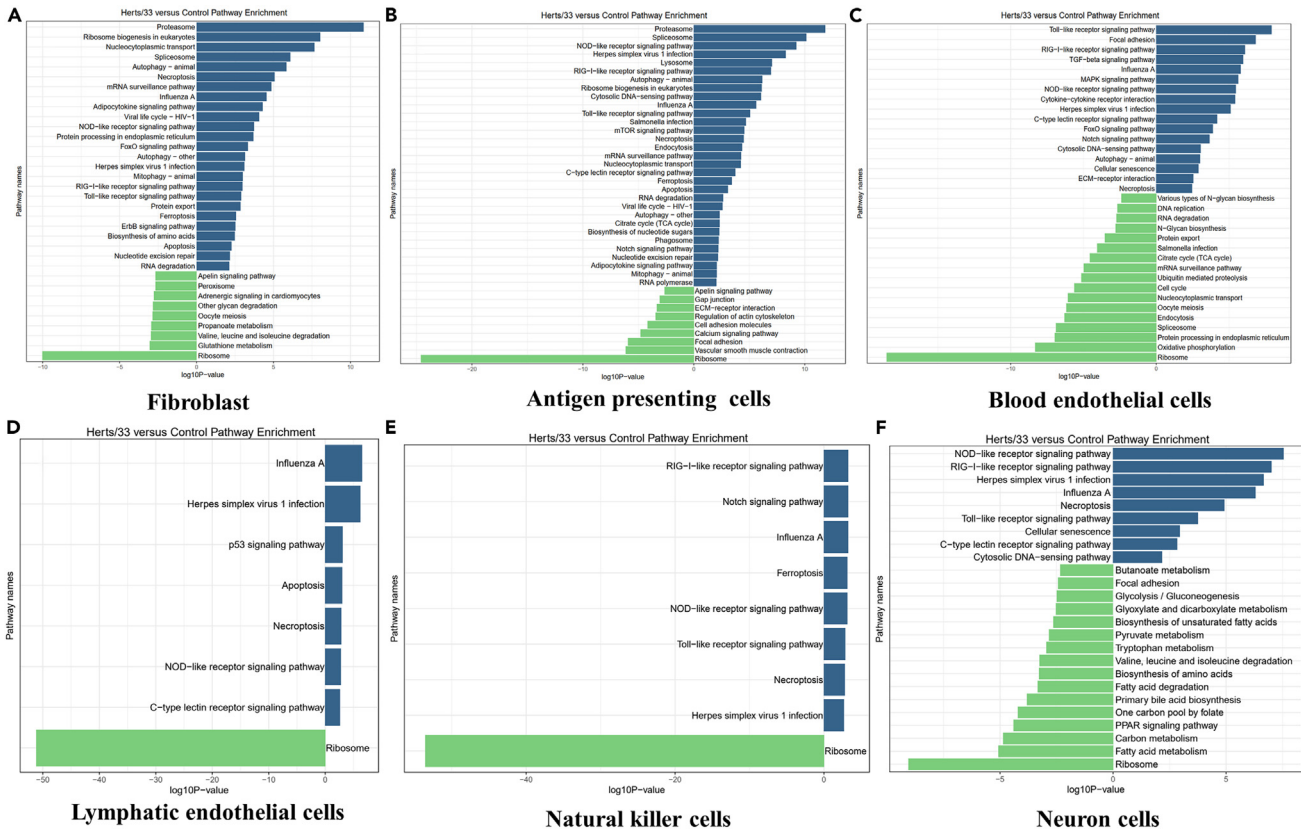


Figure 9. NDV remodel ribosomes by regulating the transcription of ribosomal proteins

KEGG pathway enrichment analyses based on differentially expressed genes in different types of cells relative to the Mock group.

(A) was from fibroblast cells, (B) from antigen-presenting cells, (C) from blood endothelial cells, (D) from lymphatic endothelial cells, (E) from natural killer cells, and (F) from neuron cells. The x axis represents the log₁₀ P-value. The y axis indicates different pathways in the enrichment analysis.

as well as the activation and manipulation of genes associated with the sphingolipid “rheostat.” Notably, the expression levels of sphingomyelin synthase genes were observed to be upregulated, driving metabolic reprogramming and facilitating the accumulation of ceramide content.²⁵ Such alterations cater to the requirements for the self-assembly of virus particles and enable optimal replication to take place (data not published). Further investigation could explore the potential relationship between the phospholipid metabolic remodeling caused by the varying levels of virulence of NDV, and the corresponding viral proteins, as well as identify the functions of these phospholipid metabolites in the replication of NDV.

According to our data, there was noteworthy variation in the replication of Herts/33 among various cell types. Endothelial cells, antigen-presenting cells, fibroblasts and neutrophils showed the greatest replication of Herts/33. Hence, it suggests that NDV replication *in vivo* displays a preference for distinct cell types (Figures 8E and 8F). It has been confirmed that endothelial cells, antigen-presenting cells, fibroblasts, and neutrophils are the primary target cells for NDV infection and invasion in chickens. Prior research has demonstrated that poultry infected with NDV exhibit neurological symptoms accompanied by severe immunosuppression.^{50–53} Our data confirmed that Herts/33 replicates actively in immune cells such as antigen-presenting cells, T lymphocytes, and neutrophils. There is also a small amount of virus replication in nerve cells (Figure 8F), which may be a potential factor for NDV to affect the normal function of immunosuppression and neural cells, leading to immune suppression and neurological symptoms.

The single-cell transcriptome analysis revealed that NDV may directly regulate ribosome protein transcription to facilitate efficient viral protein translation. This phenomenon was observed across different cell types and was not restricted to viral titers. As such, it appears that NDV infection can exert a significant impact on the host ribosome translation function. Nonetheless, our previous research conducted at the cellular level demonstrated that NDV infection inhibits cellular protein translation, and that the NP protein of NDV “hijacks” translation initiation factors, causing them to preferentially translate viral proteins.⁴ Based on our unpublished research, the original ribosome in the cell is unable to effectively translate viral proteins. To overcome this, NDV needs to remodel the ribosomes. Then, by degrading the ribosomal protein, the shape of the ribosome can be altered. This not only allows for efficient translation of viral proteins but also impedes the translation of cell proteins. In summary, NDV remodel ribosomes by regulating the transcription of ribosomal proteins.

In summary, we provide a comprehensive and in-depth understanding of the host response in chickens induced by NDV and provides a basis for further research to clarify the interaction between NDV and host plasma metabolism (Figure 12). At present, the impact of NDV

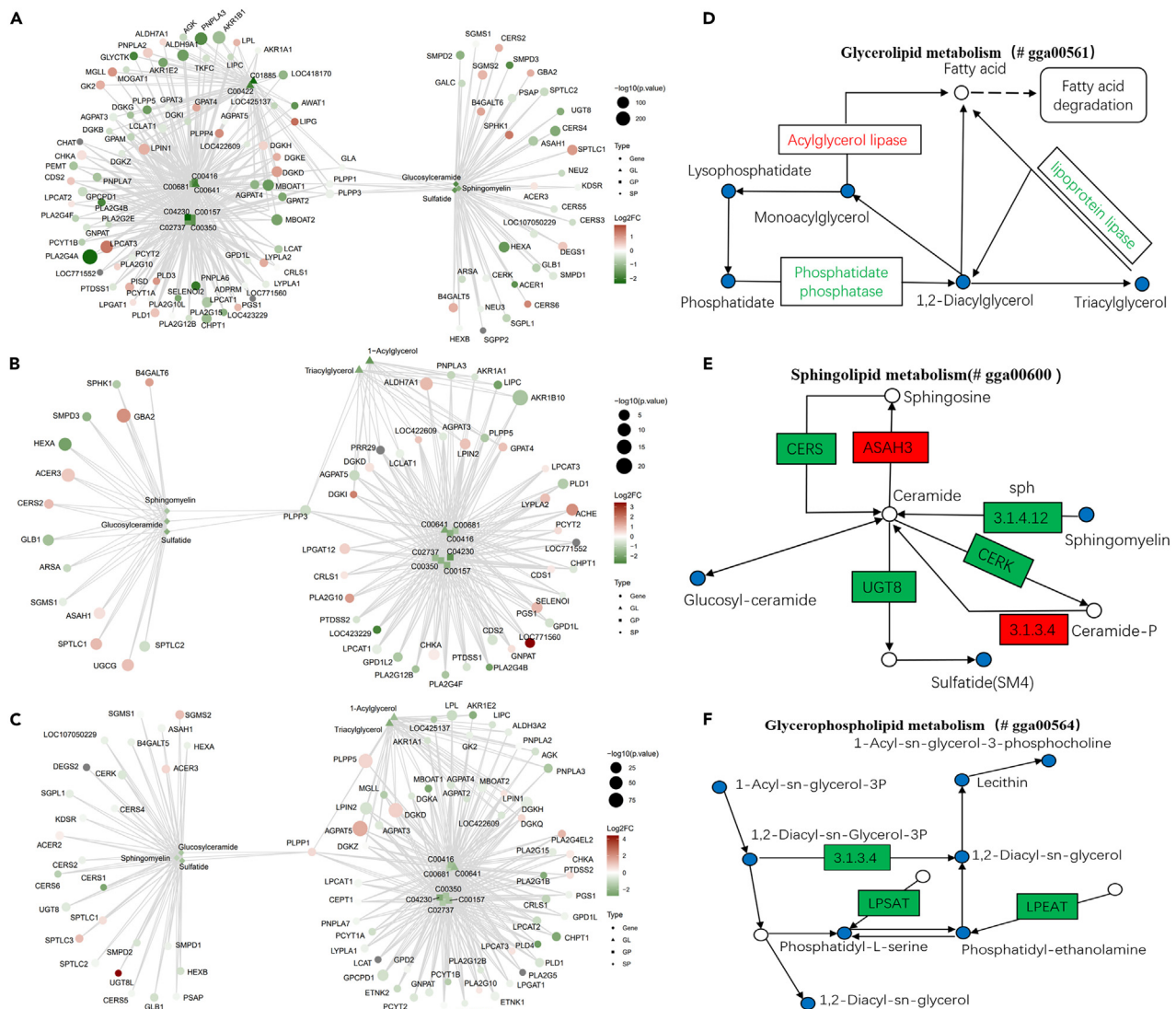


Figure 10. The relationship between transcriptome and plasma metabolome

The Wilcoxon test was used to analyze the differences in genes and metabolites between the experimental and control groups. Correlation analyses were conducted between plasma metabolites and the single-cell transcriptomes of fibroblast cells (A), epithelial cells (B), and blood endothelial cells (C). $p < 0.05$ indicated significant differences in genes and metabolites. The wiring diagram displays the metabolic pathway and differential genes or metabolites involved in the pathway. C00157, C00350, C00416, C00641, C00681, C02737, and C04230 represent the metabolites in the KEGG database as Phosphatidylcholine, Phosphatidylethanolamine, Phosphatidate, 1,2-Diacyl-sn glycerol, 1-Acyl-sn glycerol 3-phosphate, Phosphatidylserine, and 1-Acyl-sn glycerol-3-phosphocholine, respectively. Correlation analysis between metabolites and metabolic enzyme mRNA levels in three pathways of blood endothelial cells: the glycerol lipid metabolic pathway (# gga00561) (D), sphingomyelin metabolic pathway (# gga00600) (E), and glycerol phospholipid metabolic pathway (# gga00564) (F). Metabolites are represented by dots, with blue indicating downregulation, yellow indicating upregulation, and white indicating no significant difference. The metabolic enzyme mRNA is represented by a rectangle, with red indicating upregulation and green indicating downregulation.

infection on phospholipid metabolism in chickens remains uninvestigated; likewise, the metabolic markers associated with infections by NDV strains with different virulence are unknown, which hinders our understanding of the host response to the virus. Our research provides valuable insights into the demand for host cell lipid metabolism during NDV infection and sheds light on the regulatory role of NDV replication in host cell metabolic pathways. These findings lay a solid theoretical foundation for further investigations into the reprogramming of host cell metabolism by NDV. Future studies should focus on exploring the effects of phospholipid metabolites on NDV replication, and on investigating the changes in key enzymes of phospholipid metabolism during the host's response to NDV infection. The correlation between NDV's remodeling of the host's phospholipid metabolism and its pathogenic mechanisms will prove to be a promising topic for research in the future.

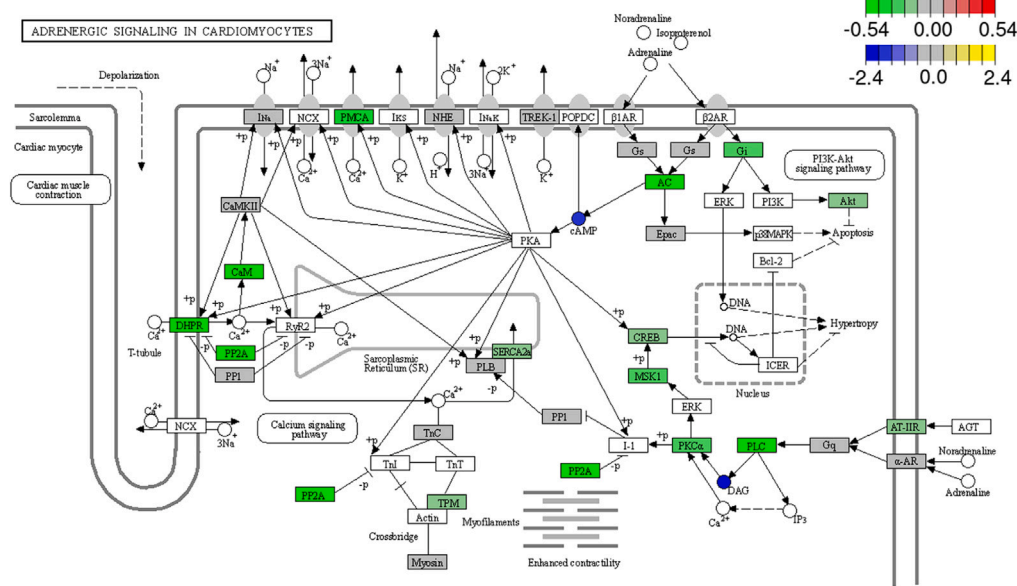


Figure 11. DAG can serve as metabolic markers for NDV infection

The hypergeometric test was used to detect the enriched P1 set of metabolic pathways associated with the gene set significantly upregulated or downregulated in the single-cell transcriptome. Similarly, the hypergeometric test was used to identify the enriched set of metabolic pathways, P2, for the significantly upregulated or downregulated metabolites in plasma metabolomics. The intersection of P1 and P2 was utilized to determine the correlated metabolites and mRNA. The rectangle denotes the gene name, where green denotes a downregulation of gene expression, red indicates an upregulation of gene expression, dots represent metabolites, blue indicates a downregulation of metabolite levels, and yellow indicates an upregulation of metabolite levels.

Limitations of the study

During viral infection, the cellular response involves the regulation of various pathways, gene and protein expression, and modulation of cellular metabolism encompassing carbohydrates, amino acids, nucleotides, and lipids. Our previous research has already elucidated the diverse metabolic remodeling induced by NDV, including host energy metabolism,¹² nucleotide metabolism,⁵ and amino acid metabolism.²⁸ For this study, our focus was on constructing a metabolic network map of plasma phospholipids during NDV infection. Nonetheless, a comprehensive and systematic investigation is necessary to fully comprehend how these metabolic factors precisely impact NDV. Additionally, further validation using cell models is indispensable in uncovering the role of phospholipid metabolites in the replication cycle of NDV.

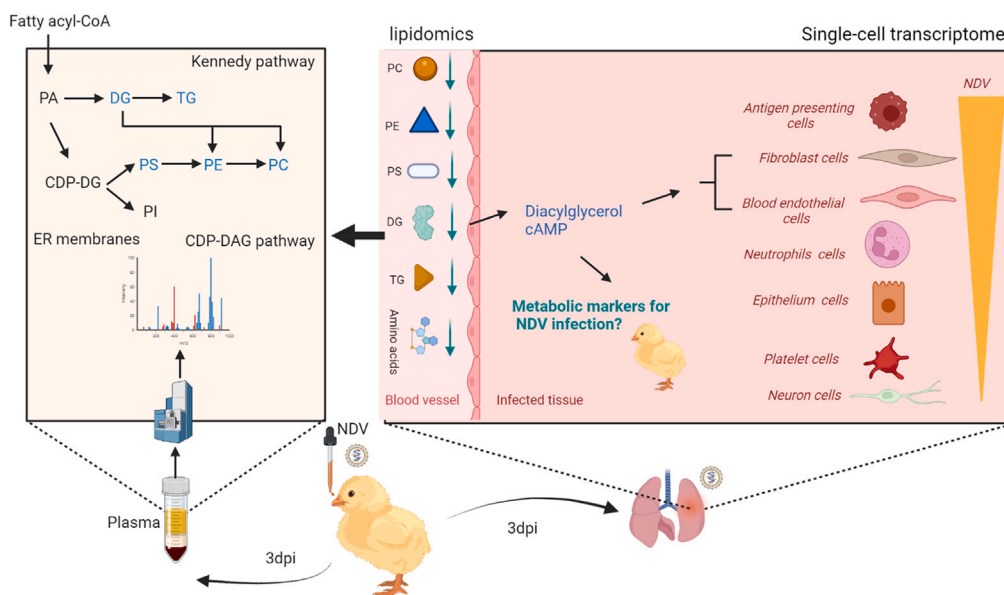


Figure 12. NDV infection remodels the plasma phospholipid metabolism in chickens

While our study demonstrated the remodeling of plasma phospholipid metabolism during NDV infection, further research is warranted to identify specific plasma phospholipid metabolites associated with NDV pathogenicity. However, conducting such an extensive experiment exceeds the scope of this study.

STAR★METHODS

Detailed methods are provided in the online version of this paper and include the following:

- KEY RESOURCES TABLE
- RESOURCE AVAILABILITY
 - Lead contact
 - Materials availability
 - Data and code availability
- EXPERIMENTAL MODEL AND STUDY PARTICIPANT DETAILS
- METHOD DETAILS
 - Methods for extraction of hydrophilic compounds
 - Methods for extraction of hydrophobic compounds
 - UPLC of hydrophilic compounds
 - UPLC of hydrophobic compounds
 - ESI-Q TRAP-MS/MS of hydrophilic compounds
 - ESI-Q TRAP-MS/MS of hydrophobic compounds
 - Single-cell transcriptome
- QUANTIFICATION AND STATISTICAL ANALYSIS

SUPPLEMENTAL INFORMATION

Supplemental information can be found online at <https://doi.org/10.1016/j.isci.2024.108962>.

ACKNOWLEDGMENTS

This work was supported by the National Key Research and Development Program of China (2022YFD1800100), the National Natural Science Foundation of China (No. 32272978, 32072868) and Natural Science Foundation of Shanghai (No. 21ZR1476800, 20ZR1469400).

AUTHOR CONTRIBUTIONS

C.D., Y.S., and X.Q. conceived the experiments and drafted the manuscript. J.D. and X.C. wrote the original draft and prepared the figures. L.T., Y.S., and Y.L. contributed reagents, materials, and discussions. Y.F. and Y.H. contributed to analysis the data. All authors read and agreed to the final published version of the manuscript.

DECLARATION OF INTERESTS

The authors declare no competing interests.

Received: August 21, 2023

Revised: December 14, 2023

Accepted: January 15, 2024

Published: January 17, 2024

REFERENCES

1. Rehman, Z.U., Qiu, X., Sun, Y., Liao, Y., Tan, L., Song, C., Yu, S., Ding, Z., Munir, M., Nair, V., et al. (2018). Vitamin E Supplementation Ameliorates Newcastle Disease Virus-Induced Oxidative Stress and Alleviates Tissue Damage in the Brains of Chickens. *Viruses* **10**, 173.
2. Brown, V.R., and Bevins, S.N. (2017). A review of virulent Newcastle disease viruses in the United States and the role of wild birds in viral persistence and spread. *Vet. Res.* **48**, 68.
3. Zhang, S., Sun, Y., Chen, H., Dai, Y., Zhan, Y., Yu, S., Qiu, X., Tan, L., Song, C., and Ding, C. (2014). Activation of the PKR/eIF2 α signaling cascade inhibits replication of Newcastle disease virus. *Virology* **47**, 11–22.
4. Gong, Y., Tang, N., Liu, P., Sun, Y., Lu, S., Liu, W., Tan, L., Song, C., Qiu, X., Liao, Y., et al. (2022). Newcastle disease virus degrades SIRT3 via PINK1-PRKN-dependent mitophagy to reprogram energy metabolism in infected cells. *Autophagy* **18**, 1503–1521.
5. Tang, N., Chen, P., Zhao, C., Liu, P., Tan, L., Song, C., Qiu, X., Liao, Y., Liu, X., Luo, T., et al. (2023). Newcastle Disease Virus Manipulates Mitochondrial MTHFD2-Mediated Nucleotide Metabolism for Virus Replication. *J. Virol.* **97**, e0001623.
6. Zhan, Y., Yu, S., Yang, S., Qiu, X., Meng, C., Tan, L., Song, C., Liao, Y., Liu, W., Sun, Y., and Ding, C. (2020). Newcastle Disease virus infection activates PI3K/Akt/mTOR and p38 MAPK/Mnk1 pathways to benefit viral mRNA translation via interaction of the viral NP protein and host eIF4E. *PLoS Pathog.* **16**, e1008610.
7. Sun, Y., Dong, L., Yu, S., Wang, X., Zheng, H., Zhang, P., Meng, C., Zhan, Y., Tan, L., Song, C., et al. (2017). Newcastle disease virus induces stable formation of stress granules to facilitate viral replication through manipulating host protein translation. *FASEB J* **31**, 1337–1353.

8. Wang, Y., Wang, R., Li, Y., Sun, Y., Song, C., Zhan, Y., Tan, L., Liao, Y., Meng, C., Qiu, X., and Ding, C. (2018). Newcastle disease virus induces G/G cell cycle arrest in asynchronously growing cells. *Virology* 520, 67–74.
9. Qu, Y., Zhan, Y., Yang, S., Ren, S., Qiu, X., Rehamn, Z.U., Tan, L., Sun, Y., Meng, C., Song, C., et al. (2018). Newcastle disease virus infection triggers HMGB1 release to promote the inflammatory response. *Virology* 525, 19–31.
10. Wang, B., Zhu, J., Li, D., Wang, Y., Zhan, Y., Tan, L., Qiu, X., Sun, Y., Song, C., Meng, C., et al. (2016). Newcastle disease virus infection induces activation of the NLRP3 inflammasome. *Virology* 496, 90–96.
11. Ren, S., Rehman, Z.U., Shi, M., Yang, B., Liu, P., Yin, Y., Qu, Y., Meng, C., Yang, Z., Gao, X., et al. (2019). Hemagglutinin-neuraminidase and fusion proteins of virulent Newcastle disease virus cooperatively disturb fusion-fission homeostasis to enhance mitochondrial function by activating the unfolded protein response of endoplasmic reticulum and mitochondrial stress. *Vet. Res.* 50, 37.
12. Gong, Y., Tang, N., Liu, P., Sun, Y., Lu, S., Liu, W., Tan, L., Song, C., Qiu, X., Liao, Y., et al. (2022). Newcastle disease virus degrades SIRT3 via PINK1-PRKN-dependent mitophagy to reprogram energy metabolism in infected cells. *Autophagy* 18, 1503–1521.
13. Sun, Y., Zheng, H., Yu, S., Ding, Y., Wu, W., Mao, X., Liao, Y., Meng, C., Ur Rehman, Z., Tan, L., et al. (2019). Newcastle Disease Virus V Protein Degrades Mitochondrial Antiviral Signaling Protein To Inhibit Host Type I Interferon Production via E3 Ubiquitin Ligase RNF5. *J. Virol.* 93, e00322-19.
14. Qiu, X., Fu, Q., Meng, C., Yu, S., Zhan, Y., Dong, L., Song, C., Sun, Y., Tan, L., Hu, S., et al. (2016). Newcastle Disease Virus V Protein Targets Phosphorylated STAT1 to Block IFN- β Signaling. *PLoS One* 11, e0148560.
15. Li, X., Feng, Y., Liu, W., Tan, L., Sun, Y., Song, C., Liao, Y., Xu, C., Ren, T., Ding, C., and Qiu, X. (2022). A Role for the Chicken Interferon-Stimulated Gene CMPK2 in the Host Response Against Virus Infection. *Front. Microbiol.* 13, 874331.
16. Tan, L., Zhang, Y., Qiao, C., Yuan, Y., Sun, Y., Qiu, X., Meng, C., Song, C., Liao, Y., Munir, M., et al. (2018). NDV entry into dendritic cells through macropinocytosis and suppression of T lymphocyte proliferation. *Virology* 518, 126–135.
17. Kan, X., Yin, Y., Song, C., Tan, L., Qiu, X., Liao, Y., Liu, W., Meng, S., Sun, Y., and Ding, C. (2021). Newcastle-disease-virus-induced ferroptosis through nutrient deprivation and ferritinophagy in tumor cells. *iScience* 24, 102837.
18. Cheng, J.-H., Sun, Y.-J., Zhang, F.-Q., Zhang, X.-R., Qiu, X.-S., Yu, L.-P., Wu, Y.-T., and Ding, C. (2016). Newcastle disease virus NP and P proteins induce autophagy via the endoplasmic reticulum stress-related unfolded protein response. *Sci. Rep.* 6, 24721.
19. Ren, S., Rehman, Z.U., Shi, M., Yang, B., Qu, Y., Yang, X.F., Shao, Q., Meng, C., Yang, Z., Gao, X., et al. (2019). Syncytia generated by hemagglutinin-neuraminidase and fusion proteins of virulent Newcastle disease virus induce complete autophagy by activating AMPK-mTORC1-ULK1 signaling. *Vet. Microbiol.* 230, 283–290.
20. Sun, Y., Yu, S., Ding, N., Meng, C., Meng, S., Zhang, S., Zhan, Y., Qiu, X., Tan, L., Chen, H., et al. (2014). Autophagy benefits the replication of Newcastle disease virus in chicken cells and tissues. *J. Virol.* 88, 525–537.
21. Rehman, Z.U., Ren, S., Yang, B., Yang, X., Butt, S.L., Afzal, A., Malik, M.I., Sun, Y., Yu, S., Meng, C., and Ding, C. (2020). Newcastle disease virus induces testicular damage and disrupts steroidogenesis in specific pathogen free roosters. *Vet. Res.* 51, 84.
22. Rehman, Z.U., Ren, S., Butt, S.L., Manzoor, Z., Iqbal, J., Anwar, M.N., Sun, Y., Qiu, X., Tan, L., Liao, Y., et al. (2021). Newcastle Disease Virus Induced Pathologies Severely Affect the Exocrine and Endocrine Functions of the Pancreas in Chickens. *Genes* 12, 495.
23. Venkata Subbaiah, K.C., Valluru, L., Rajendra, W., Ramamurthy, C., Thirunavukkarasu, C., and Subramanyam, R. (2015). Newcastle disease virus (NDV) induces protein oxidation and nitration in brain and liver of chicken: Ameliorative effect of vitamin E. *Int. J. Biochem. Cell Biol.* 64, 97–106.
24. Rehman, Z.U., Che, L., Ren, S., Liao, Y., Qiu, X., Yu, S., Sun, Y., Tan, L., Song, C., Liu, W., et al. (2018). Supplementation of Vitamin E Protects Chickens from Newcastle Disease Virus-Mediated Exacerbation of Intestinal Oxidative Stress and Tissue Damage. *Cell. Physiol. Biochem.* 47, 1655–1666.
25. Liu, W., Qiu, X., Song, C., Sun, Y., Meng, C., Liao, Y., Tan, L., Ding, Z., Liu, X., and Ding, C. (2018). Deep Sequencing-Based Transcriptome Profiling Reveals Avian Interferon-Stimulated Genes and Provides Comprehensive Insight into Newcastle Disease Virus-Induced Host Responses. *Viruses* 10, 162.
26. Meng, C., Rehman, Z.U., Liu, K., Qiu, X., Tan, L., Sun, Y., Liao, Y., Song, C., Yu, S., Ding, Z., et al. (2018). Potential of genotype VII Newcastle disease viruses to cause differential infections in chickens and ducks. *Transbound. Emerg. Dis.* 65, 1851–1862.
27. Meng, C., Qiu, X., Yu, S., Li, C., Sun, Y., Chen, Z., Liu, K., Zhang, X., Tan, L., Song, C., et al. (2016). Evolution of Newcastle Disease Virus Quasispecies Diversity and Enhanced Virulence after Passage through Chicken Air Sacs. *J. Virol.* 90, 2052–2063.
28. Liu, P., Yin, Y., Gong, Y., Qiu, X., Sun, Y., Tan, L., Song, C., Liu, W., Liao, Y., Meng, C., and Ding, C. (2019). In Vitro and In Vivo Metabolomic Profiling after Infection with Virulent Newcastle Disease Virus. *Viruses* 11, 962.
29. Chen, Y., Zhang, R., Song, Y., He, J., Sun, J., Bai, J., An, Z., Dong, L., Zhan, Q., and Abliz, Z. (2009). RRLC-MS/MS-based metabolomics combined with in-depth analysis of metabolic correlation network: finding potential biomarkers for breast cancer. *Analyst* 134, 2003–2011.
30. Thévenot, E.A., Roux, A., Xu, Y., Ezan, E., and Junot, C. (2015). Analysis of the Human Adult Urinary Metabolome Variations with Age, Body Mass Index, and Gender by Implementing a Comprehensive Workflow for Univariate and OPLS Statistical Analyses. *J. Proteome Res.* 14, 3322–3335.
31. Liu, W., Xu, Z., Qiu, Y., Qiu, X., Tan, L., Song, C., Sun, Y., Liao, Y., Liu, X., and Ding, C. (2023). Single-Cell Transcriptome Atlas of Newcastle Disease Virus in Chickens Both In Vitro and In Vivo. *Microbiol. Spectr.* 11, e0512122.
32. Wang, X., Zhou, Q., Shen, J., Yao, J., and Yang, X. (2015). Effect of difference doses of Newcastle disease vaccine immunization on growth performance, plasma variables and immune response of broilers. *J. Anim. Sci. Biotechnol.* 6, 20.
33. Ganar, K., Das, M., Sinha, S., and Kumar, S. (2014). Newcastle disease virus: current status and our understanding. *Virus Res.* 184, 71–81.
34. Dimitrov, K.M., Ferreira, H.L., Pantin-Jackwood, M.J., Taylor, T.L., Goraichuk, I.V., Crossley, B.M., Killian, M.L., Bergeson, N.H., Torchetti, M.K., Afonso, C.L., and Suarez, D.L. (2019). Pathogenicity and transmission of virulent Newcastle disease virus from the 2018-2019 California outbreak and related viruses in young and adult chickens. *Virology* 531, 203–218.
35. Rue, C.A., Susta, L., Cornax, I., Brown, C.C., Kapczynski, D.R., Suarez, D.L., King, D.J., Miller, P.J., and Afonso, C.L. (2011). Virulent Newcastle disease virus elicits a strong innate immune response in chickens. *J. Gen. Virol.* 92, 931–939.
36. Xiang, B., Zhu, W., Li, Y., Gao, P., Liang, J., Liu, D., Ding, C., Liao, M., Kang, Y., and Ren, T. (2018). Immune responses of mature chicken bone-marrow-derived dendritic cells infected with Newcastle disease virus strains with differing pathogenicity. *Arch. Virol.* 163, 1407–1417.
37. Sun, Y., Ding, N., Ding, S.S., Yu, S., Meng, C., Chen, H., Qiu, X., Zhang, S., Yu, Y., Zhan, Y., and Ding, C. (2013). Goose RIG-I functions in innate immunity against Newcastle disease virus infections. *Mol. Immunol.* 53, 321–327.
38. Xu, P., Liu, P., Zhou, C., Shi, Y., Wu, Q., Yang, Y., Li, G., Hu, G., and Guo, X. (2019). A Multi-Omics Study of Chicken Infected by Nephropathogenic Infectious Bronchitis Virus. *Viruses* 11, 1070.
39. Kuang, J., Xu, P., Shi, Y., Yang, Y., Liu, P., Chen, S., Zhou, C., Li, G., Zhuang, Y., Hu, R., et al. (2020). Nephropathogenic Infectious Bronchitis Virus Infection Altered the Metabolome Profile and Immune Function of the Bursa of Fabricius in Chicken. *Front. Vet. Sci.* 7, 628270.
40. Lin, J., Yi, X., and Zhuang, Y. (2020). Coupling metabolomics analysis and DOE optimization strategy towards enhanced IBDV production by chicken embryo fibroblast DF-1 cells. *J. Biotechnol.* 307, 114–124.
41. Chen, Y., Li, H.-W., Cong, F., and Lian, Y.X. (2021). Metabolomics profiling for identification of potential biomarkers in chickens infected with avian leukosis virus subgroup J (ALV-J). *Res. Vet. Sci.* 139, 166–171.
42. Xu, L., Wang, Z., Chen, Z., Cui, L., Liu, Z., Liang, Y., Li, X., Zhang, Y., Liu, S., and Li, H. (2022). PFT- α inhibits gallid alpha herpesvirus 1 replication by repressing host nucleotide metabolism and ATP synthesis. *Vet. Microbiol.* 269, 109435.
43. Hussein, M.A.A., Hussein, H.A.M., Thabet, A.A., Selim, K.M., Dawood, M.A., El-Adly, A.M., Wardany, A.A., Sobhy, A., Magdeldin, S., Osama, A., et al. (2022). Human Wharton's Jelly Mesenchymal Stem Cells Secretome Inhibits Human SARS-CoV-2 and Avian Infectious Bronchitis Coronaviruses. *Cells* 11, 1408.
44. Dai, J., Wang, H., Liao, Y., Tan, L., Sun, Y., Song, C., Liu, W., Ding, C., Luo, T., and Qiu, X. (2022). Non-Targeted Metabolomic Analysis of Chicken Kidneys in Response to Coronavirus IBV Infection Under Stress Induced by Dexamethasone. *Front. Cell. Infect. Microbiol.* 12, 945865.

45. Hippee, C.E., Singh, B.K., Thurman, A.L., Cooney, A.L., Pezzulo, A.A., Cattaneo, R., and Sinn, P.L. (2021). Measles virus exits human airway epithelia within dislodged metabolically active infectious centers. *PLoS Pathog.* *17*, e1009458.
46. Peng, T., Qiu, X., Tan, L., Yu, S., Yang, B., Dai, J., Liu, X., Sun, Y., Song, C., Liu, W., et al. (2022). Ubiquitination on Lysine 247 of Newcastle Disease Virus Matrix Protein Enhances Viral Replication and Virulence by Driving Nuclear-Cytoplasmic Trafficking. *J. Virol.* *96*, e0162921.
47. Chotiwan, N., Andre, B.G., Sanchez-Vargas, I., Islam, M.N., Grabowski, J.M., Hopf-Jannasch, A., Gough, E., Nakayasu, E., Blair, C.D., Belisle, J.T., et al. (2018). Dynamic remodeling of lipids coincides with dengue virus replication in the midgut of *Aedes aegypti* mosquitoes. *PLoS Pathog.* *14*, e1006853.
48. Liu, P., Tang, N., Meng, C., Yin, Y., Qiu, X., Tan, L., Sun, Y., Song, C., Liu, W., Liao, Y., et al. (2022). SLC1A3 facilitates Newcastle disease virus replication by regulating glutamine catabolism. *Virulence* *13*, 1407–1422.
49. Avota, E., de Lira, M.N., and Schneider-Schaulies, S. (2019). Sphingomyelin Breakdown in T Cells: Role of Membrane Compartmentalization in T Cell Signaling and Interference by a Pathogen. *Front. Cell Dev. Biol.* *7*, 152.
50. Ul-Rahman, A., Ishaq, H.M., Raza, M.A., and Shabbir, M.Z. (2022). Zoonotic potential of Newcastle disease virus: Old and novel perspectives related to public health. *Rev. Med. Virol.* *32*, e2246.
51. Rasoli, M., Yeap, S.K., Tan, S.W., Moeini, H., Ideris, A., Bejo, M.H., Alitheen, N.B.M., Kaiser, P., and Omar, A.R. (2014). Alteration in lymphocyte responses, cytokine and chemokine profiles in chickens infected with genotype VII and VIII velogenic Newcastle disease virus. *Comp. Immunol. Microbiol. Infect. Dis.* *37*, 11–21.
52. Kristeen-Teo, Y.W., Yeap, S.K., Tan, S.W., Omar, A.R., Ideris, A., Tan, S.G., and Alitheen, N.B. (2017). The effects of different velogenic NDV infections on the chicken bursa of Fabricius. *BMC Vet. Res.* *13*, 151.
53. Lam, K.M., Kabbur, M.B., and Eiserich, J.P. (1996). Newcastle disease virus-induced functional impairments and biochemical changes in chicken heterophils. *Vet. Immunol. Immunopathol.* *53*, 313–327.
54. Xu, J., Zhou, M., Luo, P., Yin, Z., Wang, S., Liao, T., Yang, F., Wang, Z., Yang, D., Peng, Y., et al. (2021). Plasma Metabolomic Profiling of Patients Recovered From Coronavirus Disease 2019 (COVID-19) With Pulmonary Sequelae 3 Months After Discharge. *Clin. Infect. Dis.* *73*, 2228–2239.
55. Wu, D., Shu, T., Yang, X., Song, J.-X., Zhang, M., Yao, C., Liu, W., Huang, M., Yu, Y., Yang, Q., et al. (2020). Plasma metabolomic and lipidomic alterations associated with COVID-19. *Natl. Sci. Rev.* *7*, 1157–1168.

STAR★METHODS

KEY RESOURCES TABLE

REAGENT or RESOURCE	SOURCE	IDENTIFIER
Bacterial and virus strains		
NDV strain Herts/33	China Institute of Veterinary Drug Control (Beijing, China)	N/A
NDV strain LaSota	China Institute of Veterinary Drug Control (Beijing, China)	N/A
Software and algorithms		
R (base package)	https://www.r-project.org/	
R (MetaboAnalystR)	https://www.r-project.org/	
R (base package)	https://www.r-project.org/	
R (igraph; ggraph)	https://www.r-project.org/	
R (corrplot)	https://www.r-project.org/	
R (ComplexHeatmap)	https://www.r-project.org/	
R (base package; Hmisc)	https://www.r-project.org/	
R (fmsb)	https://www.r-project.org/	
Other		
Specific pathogen-free (SPF) embryonated eggs	Beijing Boehringer Ingelheim Vital Biotechnology Co. Ltd.	

RESOURCE AVAILABILITY

Lead contact

Lead contact Further information and requests for resources and reagents should be directed to and will be fulfilled by the lead contact, Chan Ding (shoveldeen@shvri.ac.cn).

Materials availability

This study did not generate new unique reagents.

Data and code availability

All data reported in this paper will be shared by the [lead contact](#) upon request.

This paper does not report original code.

Any additional information required to reanalyze the data reported in this paper is available from the [lead contact](#) upon request.

EXPERIMENTAL MODEL AND STUDY PARTICIPANT DETAILS

All specific pathogen-free (SPF) embryonated eggs were purchased from Beijing Boehringer Ingelheim Vital Biotechnology Co. Ltd. and incubated as described previously.⁴⁴ A total of 21 healthy White Leghorns of similar weight were randomly and averagely divided into three groups of seven: mock group, Herts/33 group, LaSota group. Herts/33 group SPF chickens were challenged via an eye dropper with 200 μ L of 10^3 EID50 Herts/33; LaSota group SPF chickens were challenged via an eye dropper with 200 μ L of 10^8 50% EID50 LaSota; and PBS was the negative control. At 3 days post-infection(dpi), single-cell RNA sequencing was used to determine the transcriptional characteristics of lung tissue in chickens. The plasma sample extracts were analyzed using an LC-ESI-MS/MS system. To detect metabolites, full-spectrum metabolomics technology was used to extract and detect hydrophilic metabolites and lipids from plasma samples, following previously reported methods^{54,55} (see [Figure S1](#)). The use and care of animals were authorized by the Institutional Animal Care and Use Committee of the Shanghai Veterinary Research Institute Chinese Academy of Agricultural Sciences (SV-20201225-Y02).

METHOD DETAILS

Methods for extraction of hydrophilic compounds

Samples stored at -80° C were thawed on ice and vortexed for 10 s. Fifty microliters of sample and 300 μ L of extraction solution (ACN: methanol = 1:4, V/V) containing internal standards were added to a 2-mL microcentrifuge tube. The samples were vortexed for 3 min and

centrifuged at 12000 rpm for 10 min at 4°C. Supernatants (200 µL) were collected and placed at –20°C for 30 min, and centrifuged at 12000 rpm for 3 min (4°C). Aliquots of supernatant (180 µL) were transferred for LC-MS analysis.

Methods for extraction of hydrophobic compounds

Samples were removed from the –80°C freezer, thawed on ice and vortexed for 10 s. We mixed 50 µL of sample and 1 mL of extraction solvent (MTBE: methanol = 3:1, v/v) containing internal standard mixture. After whirling the mixture for 15 min, 200 µL of water was added, and the samples were vortexed for 1 min and centrifuged at 12,000 rpm for 10 min. The upper organic layer (200 µL) was collected and evaporated using a vacuum concentrator. The dry extract was reconstituted using 200 µL mobile phase B prior to LC-MS/MS analysis.

UPLC of hydrophilic compounds

The sample extracts were analyzed using an LC-ESI-MS/MS system (UPLC, ExionLC AD, <https://sciex.com.cn/>; MS, QTRAP System, <https://sciex.com/>). The analytical conditions were as follows. UPLC: column, Waters ACQUITY UPLC HSS T3 C18 (1.8 µm, 2.1 mm × 100 mm); column temperature, 40°C; flow rate, 0.4 mL/min; injection volume, 2 µL; solvent system, water (0.1% formic acid): acetonitrile (0.1% formic acid); gradient program, 95:5 v/v at 0 min, 10:90 V/V at 11.0 min, 10:90 V/V at 12.0 min, 95:5 V/V at 12.1 min, 95:5 V/V at 14.0 min.

UPLC of hydrophobic compounds

The sample extracts were analyzed using an LC-ESI-MS/MS system (UPLC, ExionLC AD <https://sciex.com.cn/>; MS, QTRAP System, <https://sciex.com/>). The analytical conditions were as follows, UPLC: column, Thermo Accucore C30 (2.6 µm, 2.1 mm × 100 mm internal diameter); solvent system, A: acetonitrile/water (60/40, v/v, 0.1% formic acid, 10 mmol/L ammonium formate), B: acetonitrile/isopropanol (10/90 v/v, 0.1% formic acid, 10 mmol/L ammonium formate); gradient program, A/B (80:20, v/v at 0 min, 70:30 V/V at 2 min, 40:60 v/v at 4 min, 15:85 v/v at 9 min, 10:90 v/v at 14 min, 5:95 v/v at 15.5 min, 5:95 v/v at 17.3 min, 80:20 v/v at 17.3 min, 80:20 v/v at 20 min; flow rate, 0.35 mL/min; temperature, 45°C; injection volume: 2 µL. The effluent was alternatively connected to an ESI-triple quadrupole-linear ion trap (QTRAP)-MS.

ESI-Q TRAP-MS/MS of hydrophilic compounds

LIT and triple quadrupole (QQQ) scans were acquired on a triple quadrupole-linear ion trap mass spectrometer (QTRAP), QTRAP LC-MS/MS System, equipped with an ESI Turbo Ion-Spray interface, operating in positive and negative ion mode and controlled by Analyst 1.6.3 software (Sciex). The ESI source operation parameters were as follows: source temperature 500°C; ion spray voltage (IS) 5500 V (positive), –4500 V (negative); ion source gas I (GS1), gas II (GSII), curtain gas (CUR) was set at 55, 60, and 25.0 psi, respectively; the collision gas (CAD) was high. Instrument tuning and mass calibration were performed with 10 and 100 µmol/L polypropylene glycol solutions in QQQ and LIT modes, respectively. A specific set of MRM transitions were monitored for each period according to the metabolites eluted within this period.

ESI-Q TRAP-MS/MS of hydrophobic compounds

LIT and triple quadrupole (QQQ) scans were acquired on a triple quadrupole-linear ion trap mass spectrometer (QTRAP), QTRAP LC-MS/MS System, equipped with an ESI Turbo Ion-Spray interface, operating in positive and negative ion mode and controlled by Analyst 1.6.3 software (Sciex). The ESI source operation parameters were as follows: ion source, turbo spray; source temperature 500°C; ion spray voltage (IS) 5500 V (positive), –4500 V (negative); GS1, GS2, and CUR were set at 45, 55, and 35 psi, respectively; CAD was medium. Instrument tuning and mass calibration were performed with 10 and 100 µmol/L polypropylene glycol solutions in QQQ and LIT modes, respectively. QQQ scans were acquired as MRM experiments with collision gas (nitrogen) set to 5 psi. DP and CE for individual MRM transitions were done with further DP and CE optimization. A specific set of MRM transitions were monitored for each period according to the metabolites eluted within this period.

Single-cell transcriptome

In our previous research,³¹ we detailed the steps involved in single-cell transcriptome sequencing of lung tissue from chickens infected with NDV. The process included single cell sorting, sample preparation, RNA sequencing data processing, cell type annotation, gene set variation analysis, pseudo time analysis, and NDV sequence analysis.

QUANTIFICATION AND STATISTICAL ANALYSIS

The identification of differentially enriched metabolites and metabolic pathways was as our previously described.^{28,44} In short, we used a combination of UPLC-MS/MS detection platform, self-built database (Wuhan Metware Biotechnology Co., Ltd.), and multivariate statistical analysis to study the metabolomic differences between samples. For two-group analysis, differential metabolites were determined by VIP (VIP ≥ 1) and fold change (fold change ≥ 2 or fold change ≤ 0.5). The data analysis of this study involves principal component analysis (PCA), K-Means analysis, orthogonal partial least square discriminant analysis (OPLS-DA), hierarchical cluster analysis (HCA) and Pearson correlation coefficients (PCCs). The software and version used for these analyses are shown in [key resources table](#).